Calmodulin-dependent gating of $Ca_V1.2$ calcium channels in the absence of $Ca_V\beta$ subunits

Arippa Ravindran, Qi Zong Lao, Jo Beth Harry, Parwiz Abrahimi, Evgeny Kobrinsky, and Nikolai M. Soldatov*

National Institute on Aging, National Institutes of Health, 5600 Nathan Shock Drive, Baltimore, MD 21224

Edited by Harald Reuter, University of Bern, Bern, Switzerland, and approved March 21, 2008 (received for review December 10, 2007)

It is generally accepted that to generate calcium currents in response to depolarization, $Ca_V1.2$ calcium channels require association of the pore-forming α_{1C} subunit with accessory $Ca_V\beta$ and $\alpha_2\delta$ subunits. A single calmodulin (CaM) molecule is tethered to the C-terminal α_{1C}-LA/IQ region and mediates Ca^{2+}-dependent inactivation of the channel. $Ca_V\beta$ subunits are stably associated with the α_{1C}-interaction domain site of the cytoplasmic linker between internal repeats I and II and also interact dynamically, in a Ca^{2+}-dependent manner, with the α_{1C}-IQ region. Here, we describe a surprising discovery that coexpression of exogenous CaM (CaM_{ex}) with $\alpha_{1C}/\alpha_2\delta$ in COS1 cells in the absence of $Ca_V\beta$ subunits stimulates the plasma membrane targeting of α_{1C}, facilitates calcium channel gating, and supports Ca^{2+}-dependent inactivation. Neither real-time PCR with primers complementary to monkey $Ca_V\beta$ subunits nor coimmunoprecipitation analysis with exogenous α_{1C} revealed an induction of endogenous $Ca_V\beta$ subunits that could be linked to the effect of CaM_{ex}. Coexpression of a calcium-insensitive CaM mutant CaM_{1234} also facilitated gating of $Ca_V\beta$-free $Ca_V1.2$ channels but did not support Ca^{2+}-dependent inactivation. Our results show there is a functional matchup between CaM_{ex} and $Ca_V\beta$ subunits that, in the absence of $Ca_V\beta$, renders Ca^{2+} channel gating facilitated by CaM molecules other than the one tethered to LA/IQ to support Ca^{2+}-dependent inactivation. Thus, coexpression of CaM_{ex} creates conditions when the channel gating, voltage- and Ca^{2+}-dependent inactivation, and plasma-membrane targeting occur in the absence of $Ca_V\beta$. We suggest that CaM_{ex} affects specific $Ca_V\beta$-free conformations of the channel that are not available to endogenous CaM.

plasma-membrane targeting | voltage gating

In L-type $Ca_V1.2$ calcium channels, calmodulin (CaM) plays a central role in Ca^{2+}-dependent inactivation (CDI), a physiologically important negative feedback regulated by permeating Ca^{2+} ions causing acceleration of the Ca^{2+} but not Ba^{2+} current decay. Considerable progress has been made in identifying and characterizing interactions between the pore-forming α_{1C} subunit and CaM (for the most recent review, see ref. 1). It is generally accepted that CDI is mediated by a single CaM molecule that is preassociated with the α_{1C} subunit C-terminal tail (2). The structure-functional analysis revealed two CDI-related CaM-binding sites on the $Ca_V1.2$ α_{1C} subunit C tail; one located within the segment 1572–1604 (LA) and the other confined to amino acids 1617–1636 (IQ). The mode of CaM binding to these sites depends on free Ca^{2+} concentration and hence on the occupancy of CaM by Ca^{2+}. Of particular interest is that CDI does not solely depend on the presence of these Ca^{2+} sensors and requires a number of other channel structures. These determinants crucial for CDI include a $Ca_V\beta$ subunit (3), the α_{1C} subunit N-tail (4), the determinant of slow inactivation in the pore inner region (5), and possibly the putative EF-hand locus residing in the α_{1C} subunit C-tail upstream of LA/IQ sites (6). Specific folding of these determinants supporting CDI is mediated by voltage-gated rearrangements between α_{1C} and $Ca_V\beta$ (7) and between the α_{1C} subunit cytoplasmic N- and C-tails (8). It is also known that $Ca_V\beta$ subunits bind to the α_1-interaction domain (AID) in the linker between repeats I and II of the α_{1C} subunit (9) and, in a Ca^{2+}-dependent manner, to the IQ region of the α_{1C} subunit C tail (3). The complexity of the structure and dynamics of these multifaceted determinants is not well understood. Our report provides evidence that is crucial for better understanding the functional links between these determinants, because it shows that gating of the $Ca_V\beta$-free recombinant $Ca_V1.2$ channel can be rendered by coexpression of endogenous CaM (CaM_{ex}).

Results

A number of important studies of CDI relied on coexpression of dominant-negative CaM mutants lacking Ca^{2+} binding but retaining affinity to apo-CaM sites of α_{1C} (10–12). These studies were carried out in an assumption that coexpression of CaM does not markedly change electrophysiological properties of the channel, mainly because endogenous CaM is an abundant protein reaching micromolar concentrations in the cell (13). Our study shows that CaM_{ex} does affect gating of the $Ca_V1.2$ calcium channel and facilitates it in the absence of $Ca_V\beta$ subunits.

Effect of CaM_{ex} on Electrophysiological Properties of the Recombinant $Ca_V1.2$ Calcium Channel Containing $Ca_V\beta$ Subunits. To test the effects of CaM_{ex} on the properties of Ca^{2+} channels, we used Ca^{2+} channel-free COS1 cells (4, 14). In our first set of experiments, we coexpressed $EYFP_N$-α_{1C}, $\alpha_2\delta$, and β_{2d} subunits in the presence ($+CaM_{ex}$) or absence ($-CaM_{ex}$) of $ECFP_N$-CaM. Epifluorescent images of expressing cells (Fig. 1 *A* and *B*) revealed distinct plasma membrane (PM) targeting of $EYFP_N$-α_{1C} (Fig. 1 *Aa* and *Ba*, arrows). $ECFP_N$-CaM was abundantly expressed in the cell [supporting information (SI) Fig. S1*A*] exhibited some PM targeting because it binds to the channels (Fig. 1*Ab*). Representative traces of I_{Ca} shown in Fig. 1 *A* and *B* were evoked by 600-ms test pulses in the range of 0 to +60 mV (10-mV increments). First, we found that all traces were better fitted by a single exponential function except the three traces on Fig. 1*B* ($-CaM_{ex}$) recorded at test potentials +10, +20, and +30 mV. These traces required double-exponential fitting revealing an apparent slow component of inactivation that, on average, accounted for 10–19% of the total I_{Ca} amplitude ($n = 5$). We also noticed that CaM_{ex} reduced ≈3-fold the fraction I_o of the Ca^{2+} current remaining at the end of a 600-ms test pulse (Fig. 1*C*, open circles). Although the nature of these changes is not yet clear, these data suggest that CaM_{ex} promoted inactivation of the channel. Analysis of current–voltage (*I–V*) relationships (Fig. 1*D*) showed that CaM_{ex} increased the density of I_{Ca} 2.4 ± 0.1-fold ($n = 8$). Independently on this increase, CaM_{ex} affected channel gating by shifting the maximum of *I–V* curve and $V_{0.5}$ to more negative potentials (open circles, Fig. 1*D*) and increasing

Author contributions: A.R. and Q.Z.L. contributed equally to this work; N.M.S. designed research; A.R., Q.Z.L., and J.B.H. performed research; A.R., Q.Z.L., P.A., E.K., and N.M.S. analyzed data; E.K. and N.M.S. wrote the paper.

The authors declare no conflict of interest.

This article is a PNAS Direct Submission.

*To whom correspondence should be addressed. E-mail: soldatovn@grc.nia.nih.gov.

This article contains supporting information online at www.pnas.org/cgi/content/full/0711624105/DCSupplemental.

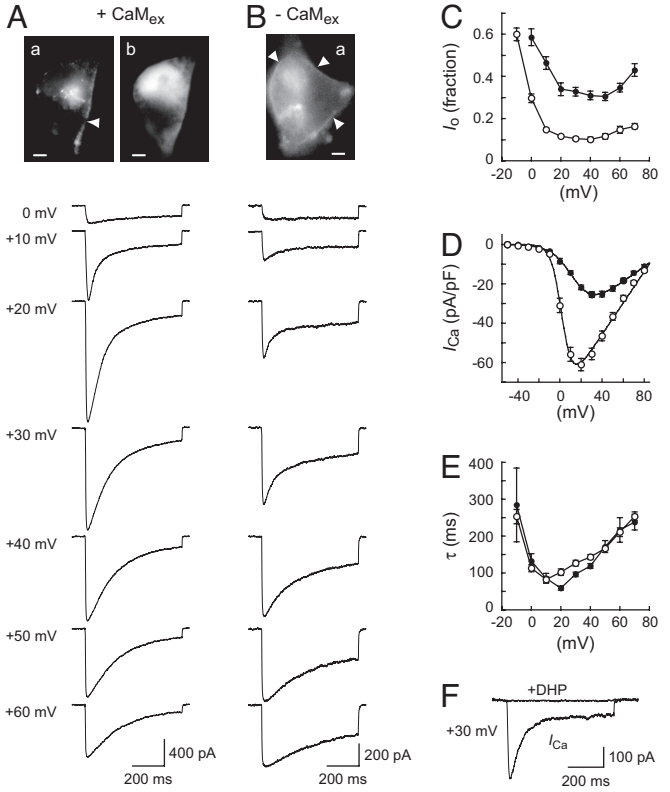

Fig. 1. Effects of CaM_{ex} on the properties of the $Ca_v1.2$ channel. The $EYFP_N$-α_{1C}, $\alpha_2\delta$ and β_{2d} subunits were expressed in COS1 cells in the presence (*A*) or absence (*B*) of $ECFP_N$-CaM. Shown are representative traces of I_{Ca} recorded in response to 600-ms steps to indicated test potentials (V_t) from the holding potential $V_h = -90$ mV. (*a* and *b*) Epifluorescent images of the expressing cells showing distribution of $EYFP_N$-α_{1C} and $ECFP_N$-CaM and obtained with the YFP and CFP filters, respectively. (Scale bars, 4 μm.) Arrows point to PM targeting of $EYFP_N$-α_{1C}. Inactivation time constants (τ) were determined from the fitting of I_{Ca} decay by an exponential function: $I(t) = I_\infty + I \times \exp(-t/\tau)$, where I_∞ is the steady-state amplitude of the current, I is apparent inactivating component of the initial current. I_o is the sustained current component determined as the ratio of steady state to peak current amplitudes. (*C*) Voltage dependence of the sustained component I_o of the I_{Ca} inactivation. (*D*) The averaged *I–V* curves for I_{Ca} recorded in the absence (filled circles) or presence of coexpressed CaM (open circles). Currents were measured with 30-s intervals between 0.6-s test pulses in the range of -60 to $+80$ mV applied with 10-mV increments from $V_h = -90$ mV. Smooth lines represent fitting by equation $I_{Ca} = G_{max}(V - E_{rev})/(1 + \exp[(V - V_{0.5})/k_{I-V}])$, where G_{max} is maximum conductance, E_{rev} is the approximated reversal potential, $V_{0.5}$ is voltage at 50% of I_{Ca} activation, and k_{I-V} is slope factor. $Ca_v1.2$: $V_{0.5} = 14.6 \pm 0.6$, $k_{I-V} = -9.9 \pm 0.3$, $E_{rev} = 105.2 \pm 3.5$ mV ($n = 5$); $Ca_v1.2 + CaM_{ex}$: $V_{0.5} = 2.4 \pm 0.6$, $k_{I-V} = -5.0 \pm 0.5$, $E_{rev} = 93.9 \pm 1.3$ mV ($n = 8$). (*E*) Voltage dependence of τ for I_{Ca} recorded in the absence (filled circles) or presence of CaM_{ex} (open circles). All error bars reflect SEM. (*F*) Inhibition of I_{Ca} through the $EYFP_N$-α_{1C}/$\alpha_2\delta$/β_{2d}/CaM_{ex} channel by 2 μM (+)PN200–110. $V_h = -90$ mV, $V_t = +30$ mV.

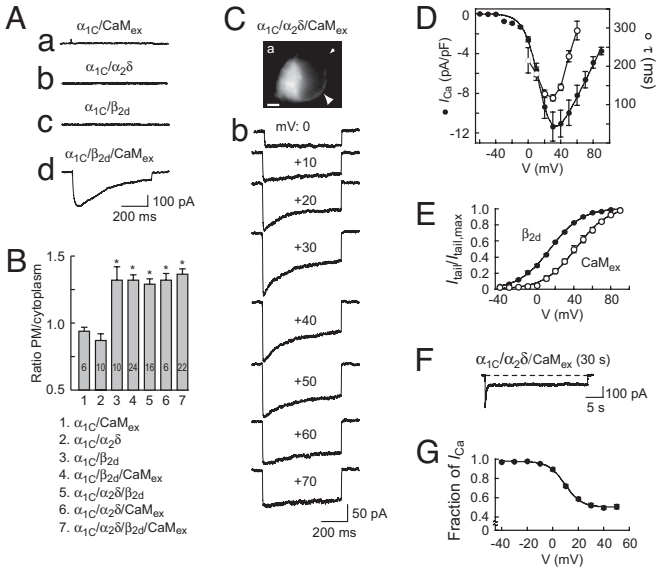

Fig. 2. Effects of CaM_{ex} on the properties of the β-deficient $Ca_v1.2$ channel. (*A*) Ca^{2+} channel activity in COS1 cells expressing $EYFP_N$-α_{1C} and CaM_{ex} (*a*), $\alpha_2\delta$ (*b*), β_{2d} (*c*), or β_{2d} +CaM_{ex} (*d*). Shown are representative traces ($n = 5$–10) of maximal I_{Ca} evoked by 600-ms test pulses to +20 mV (*a* and *c*), +30 mV (*b*), or +50 mV (*d*) applied from $V_h = -90$ mV. (*B*) Relative distribution of $EYFP_N$-α_{1C} in PM over the cytoplasm in the presence of CaM_{ex} (*1*), $\alpha_2\delta$ (2), β_{2d} (3), β_{2d} + CaM_{ex} (4), $\alpha_2\delta + \beta_{2d}$ (5), $\alpha_2\delta$ + CaM_{ex} (6), or $\alpha_2\delta + \beta_{2d}$ + CaM_{ex} (7). The ratio of fluorescence intensity in PM over the area underneath PM was averaged after background subtraction in each cell. The ratio <1.0 indicates lack of significant α_{1C} PM targeting. ANOVA statistical analysis with Tukey–Kramer multiple comparison test was applied. The number of tested cells is shown in the bars. *, $P < 0.05$. (*C*) Effect of CaM_{ex} on PM targeting and activity of Ca^{2+} channels in COS1 cells expressing $EYFP_N$-α_{1C}, $\alpha_2\delta$. (*a*) Whole-cell EYFP fluorescence. (Scale bar, 4 μm.) (*b*) Representative traces of I_{Ca} recorded in response to the indicated 600-ms test pulses ($V_h = -90$ mV). (*D*) Average *I–V* relationship for I_{Ca} through the $\alpha_{1C}/\alpha_2\delta/CaM_{ex}$ channel (filled circles) coplotted with the voltage dependence of τ (open circles). $V_{0.5} = 15.8 \pm 0.8$, $k_{I-V} = -9.1 \pm 0.5$, $E_{rev} = 110.3 \pm 2.2$ mV ($n = 5$). (*E*) Voltage dependence of activation of $EYFP_N$-$\alpha_{1C}/\alpha_2\delta$ coexpressed with β_{2d} (filled circles, $n = 7$) or CaM_{ex} (open circles, $n = 9$). Ca^{2+} tail currents (I_{tail}) were recorded after repolarization for 10 ms to -50 mV following V_t from -40 to +90 mV applied from $V_h = -90$ mV for 20 ms. I_{tail} were normalized to the peak I_{tail} ($I_{tail,max}$) and fitted with a Boltzmann equation: $I_{tail}/I_{tail,max} = (A_1 - A_2)/[1 + \exp(V - V_{a,50})/k_a] + A_2$, were $V_{a,50}$ is the half-maximal voltage for current activation, k_a is the slope factor, A_1 and A_2 represent proportion of fully activated and nonactivated current. (*F*) Representative trace of I_{Ca} through the CaM_{ex}-activated β-deficient $Ca_v1.2$ channel evoked by V_t to +40 mV applied from $V_h = -90$ mV for 30 s. (*G*) Averaged steady-state inactivation curve for I_{Ca} through the $EYFP_N$-$\alpha_{1C}/\alpha_2\delta$/CaM channel ($n = 5$). One-second conditioning prepulses were applied from $V_h = -90$ mV (up to +50 mV, 10-mV increments) followed by a 100-ms V_t to +40 mV. The intervals between each cycle were 15 s. The peak current amplitudes in each curve were normalized to the maximum value determined in the range of -40 to +50 mV. The curves were fitted (smooth line) by Boltzmann function: $I = A + B/(1 + \exp[(V - V_{0.5,in})/k])$, where A (0.50 ± 0.01) and B are fractions of noninactivating and inactivating currents, respectively, V is the conditioning prepulse voltage, $V_{0.5,in} = 10.3 \pm 0.6$ mV is the voltage at half-maximum of inactivation, and $k = 5.4 \pm 0.5$ is a slope factor.

k_{I-V} as compared with the control channel expressed in the absence of CaM_{ex} (closed circles). However, the kinetics of I_{Ca} inactivation was not significantly changed by CaM_{ex} (Fig. 1*E*) and in both cases exhibited a U-shaped dependence of the time constant of inactivation (τ) on membrane voltage characteristic for CDI that is accelerated with larger I_{Ca} (15). There was a 10-mV shift of the maximum of the τ-*V* relation to more negative potentials (open circles) corresponding to the shift of the *I–V* maximum caused by CaM_{ex}. Finally, the CaM_{ex}-modulated channel was fully inhibited by a specific L-type Ca^{2+} channel blocker PN200–110 (2 μM, Fig. 1*F*). Taken together, these results revealed that CaM_{ex} modified channel gating and augmented I_{Ca} through the $Ca_v1.2$ calcium channel.

CaM_{ex} Supports Calcium Channel Gating on Coexpression with $\alpha_{1C}/\alpha_2\delta$ in COS1 Cells in the Absence of $Ca_v\beta$ Subunits. In the absence of $Ca_v\beta$ subunits, coexpression of α_{1C} with either CaM_{ex} or $\alpha_2\delta$ generated silent channels (Fig. 2 *A a* and *b*). This is believed to be a result of poor PM targeting by the $Ca_v\beta$-deficient $Ca_v1.2$ channel and an inhibition of the channel by the α_{1C} subunit N tail (for details, see ref. 4). Lack of significant PM targeting was confirmed by the quantitative analysis of distribution of α_{1C} between PM and the cytoplasm (Fig. 2*B*, columns 1 and 2). Expression of β_{2d} in the absence of $\alpha_2\delta$ stimulated PM

targeting of α_{1C} (Fig. 2*B*, column 3), but the channel remained silent (Fig. 2*Ac*) unless CaM_{ex} was coexpressed (Fig. 2*Ad*). Thus, CaM_{ex} facilitates voltage gating of the $Ca_v1.2$ channel.

In the absence of $Ca_v\beta$, CaM_{ex} enhanced PM targeting of $\alpha_{1C}/\alpha_2\delta$ (Fig. 2*Ca*, arrows) as effectively as that by $\beta_{2d} \pm \alpha_2\delta$ (Fig. 2*B*, columns 3, 5, 6), but there was no synergy between CaM_{ex} and β_{2d} with or without $\alpha_2\delta$ (columns 4, 7). Coexpression of $ECFP_N$-CaM_{ex} with $\alpha_{1C}/\alpha_2\delta$ recovered gating of the $Ca_v\beta$-deficient channel that retained sensitivity to PN200–110 (Fig. S2*A*). $ECFP_N$-tagging does not interfere with this effect of CaM_{ex} (see Fig. S2 *B* and *C*). Fig. 2*C* shows a collection of representative traces of I_{Ca} elicited by 600-ms test pulses to indicated voltages applied from $V_h = -90$ mV. The corresponding averaged *I–V* relationship and deduced voltage-dependent characteristics are presented in Fig. 2*D*. The threshold of activation of I_{Ca} was ≈ -40 mV, and the voltage that elicited the maximal I_{Ca} (+40 mV) was shifted by 10 mV to more positive potentials as compared with β_{2d} (Fig. 1*D*). Analysis of tail currents (16) showed a significant difference in the activation parameters with β_{2d}. Half-activation potential $V_{a,0.5}$ was shifted from 14.6 ± 0.3 mV ($n = 7$) for β_{2d} to 42.5 ± 1.1 mV ($n = 9$) for CaM_{ex} without notable change in the slope factor [k_a = 17.1 ± 0.3 (β_{2d}) and 17.4 ± 0.7 (CaM_{ex})] (Fig. 2*E*). This result confirms that CaM_{ex} affects $Ca_v1.2$ channel gating in the absence of $Ca_v\beta$. An intriguing parallel between the effects of $Ca_v\beta$ and CaM_{ex} on channel gating is that both critically depend on the presence of $\alpha_2\delta$. Neither β_{2d} nor CaM_{ex} supported appreciable currents in the absence of $\alpha_2\delta$ (Fig. 2*A*).

An interesting feature of the $Ca_v\beta$-deficient channel activated by CaM_{ex} is its notably slow inactivation. When the test pulse duration was prolonged to 30 s (Fig. 2*F*), approximately one-third of the maximal I_{Ca} did not show appreciable decay. This result is in agreement with the steady-state inactivation analysis (Fig. 2*G*) indicating there is a large fraction of noninactivating channels. A monoexponential fitting of the inactivation time course (Fig. 2*D*, open circles) revealed a markedly slower inactivation (τ = 117 ± 8 ms for the peak current at +30 mV, $n = 5$) as compared with the $\alpha_{1C}/\alpha_2\delta/\beta_{2d}$ channel (59 ± 6 ms at +20 mV, $n = 5$) and a distinct U-shaped voltage dependence of τ reflecting CDI. Thus, lack of $Ca_v\beta$ is not crucial for CDI on coexpression of α_{1C} and $\alpha_2\delta$ with CaM_{ex}. However, CDI accounts for only a fraction of I_{Ca} decay in the $Ca_v\beta$-free channel.

Ca^{2+} Dependence of the Channel Modulation by CaM_{ex}. To further explore Ca^{2+} dependence of the CaM_{ex} effects, we inhibited Ca^{2+}-induced molecular rearrangements of CaM by replacing Ca^{2+} for Ba^{2+} as the charge carrier. Fig. 3*A* shows a representative trace of I_{Ba} recorded in response to a 600-ms test depolarization to +30 mV corresponding to the maximum of the *I–V* curve (Fig. 3*B*). We found that I_{Ba} decays with kinetics slower than that of I_{Ca} through this channel (Fig. 3*A*; see the superimposed gray trace scaled to the same amplitude), confirming that CDI is responsible in part for inactivation of I_{Ca} in this channel. Accordingly, the steady-state inactivation curve (Fig. 3*C*) showed that the voltage-dependent availability of Ca^{2+} channels (0.67 ± 0.01, $n = 5$) increased by ≈34% in the Ba^{2+} bath medium as compared with Ca^{2+} (Fig. 2*G*). Thus, the Ba^{2+} experiment showed that CaM_{ex}-induced gating of the channel does not require Ca^{2+} and is not due to enhanced Ca^{2+} buffering by CaM_{ex}.

We then coexpressed α_{1C} and $\alpha_2\delta$ in COS1 cells with the Ca^{2+}-insensitive mutant CaM_{1234} (17). This dominant-negative CaM mutant was shown to inhibit CDI of $Ca_v1.2$ calcium channels (10, 12) while retaining ability to bind to the CDI site of the α_{1C} subunit (11). Similar to CaM_{ex}, coexpression of CaM_{1234} enhanced PM targeting of $EYFP_N$-α_{1C} (Fig. 4*A*, arrows). Both *I–V* (Fig. 4*B*) and steady-state inactivation curves (Fig. 4*C*) for I_{Ca} measured with CaM_{1234} were not significantly

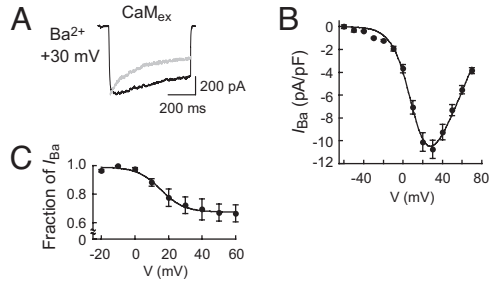

Fig. 3. Effect of the replacement of Ca^{2+} for Ba^{2+} as the charge carrier through the $EYFP_N$-$\alpha_{1C}/\alpha_2\delta$ channel modulated by CaM_{ex}. The $EYFP_N$-α_{1C} and $\alpha_2\delta$ subunits were coexpressed in COS1 cells with $ECFP_N$-CaM. (*A*) Representative trace of the maximum I_{Ba} evoked by $V_t = +30$-mV applied for 600 ms from $V_h = -90$ mV. For comparison, gray line shows the decay portion of the I_{Ca} trace (+30 mV, see Fig. 2*C*) scaled to the same amplitude. (*B*) The averaged normalized *I–V* curve: $V_{0.5} = 11.4 \pm 1.5$, $k_{I-V} = -9.4 \pm 0.7$, $E_{rev} = 93.5 \pm 3.7$ mV ($n = 18$). (*C*) Averaged steady-state inactivation curve for I_{Ba}: $A = 0.67 \pm 0.01$, $V_{0.5,in} = 15.4 \pm 1.6$ mV; $k = 6.9 \pm 1.4$ ($n = 5$).

different from those obtained with CaM_{ex} (compare statistics in legends to Figs. 2 and 4). The activation curve (Fig. 4*D*) was shifted from that for β_{2d} by ≈15 mV to more positive potentials. Differences of the activation parameters for CaM_{1234} ($V_{a,0.5}$ = 31.0 ± 0.4 mV, $k_a = 15.2 \pm 0.3$, $n = 4$) with CaM_{ex} (Fig. 2*E*) may be due to the CaM_{1234}-induced inhibition of CDI that is known to affect voltage dependence of the channel (17). Indeed, experiment with CaM_{1234} did not reveal a U shape of τ-*V* dependence (Fig. 4*B*). Respectively, inactivation of I_{Ca} through the $\alpha_{1C}/\alpha_2\delta/CaM_{1234}$ channel recorded at the peak of the *I–V* relationship (Fig. 4*E*) was slower than that with CaM_{ex} (gray trace) and matched closely inactivation of I_{Ba} (Fig. 3*A*). Taken together, the results of Ba^{2+} and CaM_{1234} experiments suggest that the ability of CaM_{ex} to support the $Ca_v\beta$-free $Ca_v1.2$ channel

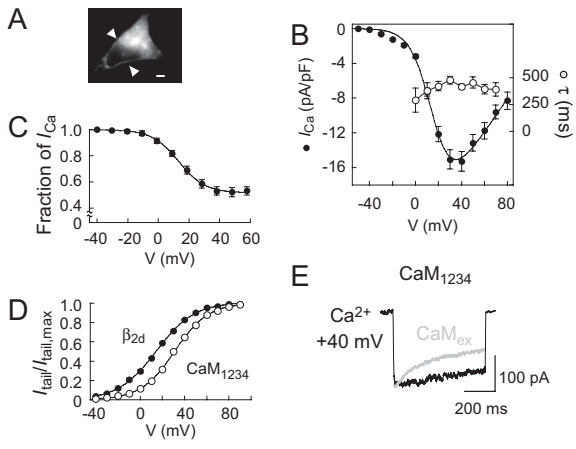

Fig. 4. Ca^{2+}-insensitive CaM_{1234} mutant supports gating of the $Ca_v\beta$-subunit-deficient $Ca_v1.2$ calcium channel. The $EYFP_N$-α_{1C} and $\alpha_2\delta$ subunits were coexpressed in COS1 cells with CaM_{1234}. (*A*) Epifluorescent image of an expressing cell showing PM targeting of $EYFP_N$-α_{1C} (arrows). (Scale bar, 4 μm.) (*B*) The averaged *I–V* curve (filled circles) coplotted with voltage dependence of τ for I_{Ca} (open circles): $V_{0.5} = 15.8 \pm 1.0$, $k_{I-V} = -9.1 \pm 0.6$, $E_{rev} = 120.8 \pm 3.5$ mV (n = 7). (*C*) The averaged steady-state inactivation curve for I_{Ca}: $A = 0.52 \pm 0.01$, $V_{0.5,in} = 14.5 \pm 0.4$ mV; $k = 8.8 \pm 0.4$ ($n = 6$). (*D*) Averaged normalized voltage dependence of activation of I_{Ca} through $\alpha_{1C}/\alpha_2\delta$ coexpressed with β_{2d} (filled circles; $n = 4$) or CaM_{1234} (open circles; $n = 4$). (*E*) Representative trace of the maximum I_{Ca} activated by V_t to + 40 mV applied for 600 ms from $V_h = -90$ mV. For comparison, the gray line shows a decay portion of I_{Ca} through the β-deficient $\alpha_{1C}/\alpha_2\delta/CaM_{ex}$ channel evoked by $V_t = +40$-mV (for original trace, see Fig. 2*C*).

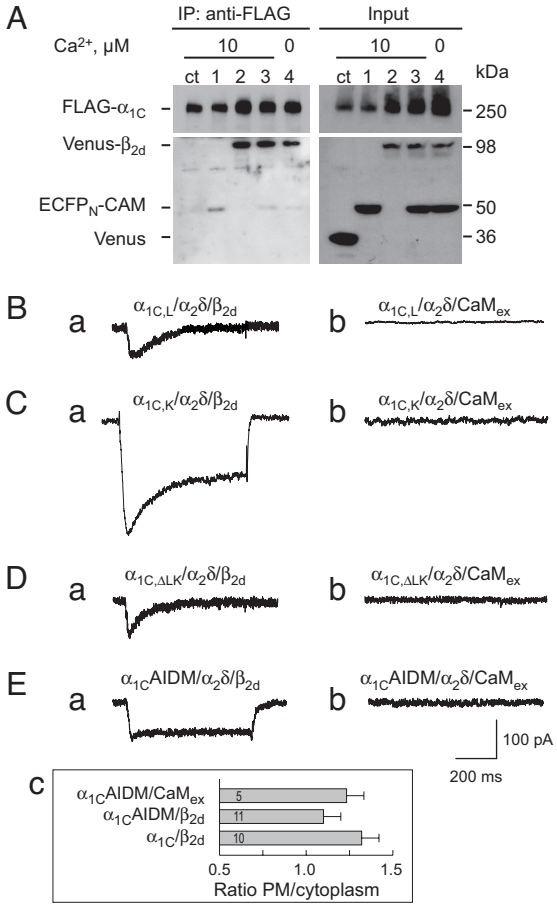

Fig. 5. Competition between CaM_{ex} and $Ca_v\beta$ for interaction with $\alpha_{1C}/\alpha_2\delta$. (*A*) Western blot analysis (representing two independent experiments) of coimmunoprecipitation (IP) of CaM_{ex} with α_{1C} in the absence (lane 1) or presence (2-4) of β_{2d}. $FLAG_N$-α_{1C} and $\alpha_2\delta$ were coexpressed in COS1 cells with Venus (ct, control), $ECFP_N$-CaM (1), Venus-β_{2d} (2), or $ECFP_N$-CaM + Venus-β_{2d} (3, 4) (*Right*). Cells were lysed in the presence of 10 μM (ct, 1-3) or zero Ca^{2+} (4) and coIP with anti-FLAG Ab (*Left*). The expressed proteins (see *Left*) were analyzed with anti-FLAG (*Upper*) or anti-LC Ab (*Lower*). Molecular mass standards (in kDa) are indicated on the right. (*B–E*) Inhibition of CaM_{ex} modulation of the $Ca_v\beta$-free Ca^{2+} channels by mutation of major CDI- or $Ca_v\beta$-related α_{1C} functional motifs. (*B*) $\alpha_{1C,L}$ (LA-), (*C*) $\alpha_{1C,K}$ (IQ-), (*D*) $\alpha_{1C,\Delta LK}$ (LA+IQ-deficient), or (*E*) $mVenus_N$-α_{1C}AIDM α_{1C} subunits were coexpressed with $\alpha_2\delta$ and either $ECFP_N$-CaM or β_{2d} (*a*) or (*b*). Shown are representative traces (n = 3–10) of maximal I_{Ca} recorded in response to $V_t = +30$ (*C* and *D*) or +20 mV (*B* and *E*). $V_h = -90$ mV. (*c*) Distribution of $EYFP_N$-α_{1C}AIDM between PM and the cytoplasm in the presence of CaM_{ex} or β_{2d} as compared with that for $EYFP_N$-α_{1C} in the presence of β_{2d} (see Fig. 2*B*). Number of tested cells is shown in the bars. *, $P < 0.05$.

gating is not associated with the Ca^{2+}-binding property of CaM and its role in CDI.

Molecular Correlates of the CaM_{ex}-Dependent Gating of $Ca_v\beta$-Deficient Channels. Coimmunoprecipitation analyses have shown that CaM_{ex} pulled down with α_{1C}, whereas endogenous CaM was not detectable in coimmunoprecipitated protein mixture (Fig. S1*B*). Because binding of CaM_{ex} to α_{1C} was inhibited in the presence of $Ca_v\beta$ with 0 or 10 μM Ca^{2+} (Fig. 5*A*), we focused on the role of known $Ca_v\beta$ determinants of α_{1C} (AID and IQ) in the effect of CaM_{ex}. LA and IQ are the primary binding sites of CaM supporting CDI. It was shown that mutation or deletion of LA and/or IQ deprives the channel of CDI but does not inhibit the modulation of $Ca_v1.2$ gating by $Ca_v\beta$ (18–20), as can be seen in Fig. 5 *Ba–Da*. However, the

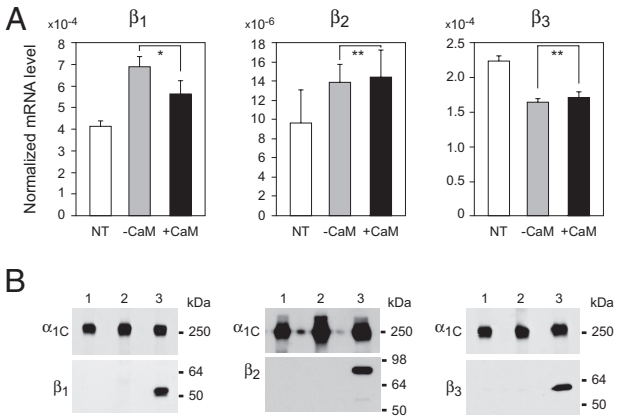

Fig. 6. CaM_{ex} does not induce endogenous $Ca_v\beta$ subunits in COS1 cells. (*A*) Lack of effect of CaM_{ex} on relative mRNA levels of endogenous $Ca_v\beta$ in COS1 cells. Each image represents a real-time PCR assessment (mean ± SEM, $n = 5$) of the mRNA levels (relative to GAPDH mRNA) of three major $Ca_v\beta$ subunits in nontransfected COS1 cells (NT) or those coexpressing α_{1C} and $\alpha_2\delta$ with the EYFP mutant Venus (−CaM) or $ECFP_N$-CaM (+CaM) under standard conditions used for electrophysiological experiments (*Methods*). PCR primers were designed to invariant exons of the monkey β_1, β_2, and β_3 subunit genes. *, $P < 0.05$; **, $P > 0.05$. (*B*) Lack of effect of CaM_{ex} on endogenous $Ca_v\beta$ binding to α_{1C} revealed by coimmunoprecipitation analysis. $FLAG_N$-α_{1C} and $\alpha_2\delta$ were coexpressed in ≈10^6 COS1 cells with (lane 1) Venus, (lane 2) $ECFP_N$-CaM, or (lane 3) human β_{1b} (GenBank accession no. M92302, *a*), β_{2d} (GenBank accession no. AF423191, *b*), or β_3 subunit (GenBank accession no. X76555, *c*). α_{1C} was identified on Western blot by anti-FLAG Ab (*Upper*). $Ca_v\beta$ subunits were identified (*Lower*) by Abs generated against rat/rabbit/human epitopes common with monkey: β_1 (GenBank accession no. XM_001085813, monkey amino acids 19–34, *a*), β_2 (GenBank accession no. XM_001092601, 387–410, *b*), and β_3 (GenBank accession no. XM_001102938, 477–491, *c*). Molecular mass calibration in kDa is shown at right.

LA- ($\alpha_{1C,L}$), IQ- ($\alpha_{1C,K}$), or LA+IQ-deficient ($\alpha_{1C,\Delta LK}$) channels showed no activity in the absence of $Ca_v\beta$ irrespectively of coexpression of CaM_{ex} (Fig. 5 *Bb–Db*). Thus, determinants of CDI are crucial for the CaM_{ex}-dependent gating of the $Ca_v\beta$-deficient channel.

We then tested whether the CaM_{ex}-supported gating depends on AID. The crucial amino acids (Asp^{433}, Gly^{436}, Tyr^{437}, and Trp^{440}) in AID (21–23) were converted to alanines, and the α_{1C}AIDM mutant was coexpressed with $\alpha_2\delta$ and β_{2d} (Fig. 5*E*). Western blot analysis unequivocally confirmed the lack of binding between β_{2d} and the mutated AID (33), but β_{2d} retained binding to IQ (3), and the channel generated I_{Ca} in response to V_t = +30-mV (Fig. 5*Ea*). When α_{1C}AIDM and $\alpha_2\delta$ were coexpressed with CaM_{ex} in the absence of $Ca_v\beta$, the channel remained silent in response to V_t in the range of −40 to +80 mV (see an exemplar trace on Fig. 5*Eb*), despite distinct PM localization (Fig. 5*Ec*). These data suggest that AID is also responsible for the CaM_{ex}-dependent gating, and its mutation ablates the effect of CaM_{ex}. Taken together, our results provide evidences that the CaM_{ex}-dependent gating of the $Ca_v\beta$-deficient channel is mediated by interdependent determinants AID and LA/IQ of α_{1C} involved in the regulation of the channel by $Ca_v\beta$.

Assessment of Endogenous $Ca_v\beta$ Subunits. Previously, little or no endogenous $Ca_v\beta$ immunoreactivity was observed in COS7 cells even when α_{1C} was expressed (14). To test whether CaM_{ex} may induce the expression of endogenous $Ca_v\beta$ subunits, we carried out a comparative qPCR analysis of the monkey β_1, β_2, and β_3 transcripts in nontransfected COS1 cells (NT) and those coexpressing the α_{1C} and $\alpha_2\delta$ subunits with Venus (−CaM) or $ECFP_N$-CaM (+CaM) (Fig. 6*A*). A less common β_4 (known to be expressed in the brain and cochlea) was not analyzed by

PHYSIOLOGY

qPCR, because the structure of monkey β_4 is not known. We found that CaM_{ex} did not induce mRNA of endogenous β_2 and β_3 subunits, and in the case of β_1, even significantly reduced it. Two independent coimmunoprecipitation analyses with α_{1C} confirmed this result and showed (Fig. 6*B*) that Abs to common epitopes of rabbit/rat/human and monkey $Ca_v\beta$ subunits did not detect appreciable binding of α_{1C} to endogenous $Ca_v\beta$ in the absence (lanes 1) or presence of CaM_{ex} (lanes 2), as compared with a respective exogenous $Ca_v\beta$ (lanes 3). Endogenous β_4 in COS1 cells was not detectable with anti-β_4 polyclonal Ab (data not shown), thus confirming a similar earlier assessment (14). In conclusion, these data and lack of appreciable Ca^{2+} or Ba^{2+} currents on coexpression of α_{1C} and $\alpha_2\delta$ subunits without CaM_{ex} (Fig. 3*A*) strongly suggest that the channel activity rendered by CaM_{ex} is not due to an induction of endogenous $Ca_v\beta$ subunits.

Discussion

Although many details of the mechanism of CDI were understood after the discovery of the LA/IQ determinants in α_{1C} and the CDI-supporting function of CaM (1), much less is known regarding the role of $Ca_v\beta$ subunits in the regulation of the $Ca_v1.2$ channel by CaM. Our findings give a previously uncharacterized perspective on the role of CaM in $Ca_v1.2$ channels by establishing that, in the absence of $Ca_v\beta$ subunits, CaM_{ex} exerts $Ca_v\beta$-like functions in the channel, including the stimulation of PM targeting and support of the channel gating (Fig. 2). These effects of CaM_{ex} do not rely on endogenous $Ca_v\beta$ (Fig. 6) and require $\alpha_2\delta$ and α_{1C} with fully functional LA/IQ and AID motifs (Fig. 5). The ability of the dominant-negative CaM_{1234} to support $Ca_v\beta$-free gating (Fig. 4) indicates that the functional effect is not related to Ca^{2+} binding to CaM_{ex}.

Perhaps the most surprising result from our study is that the functions, traditionally linked to $Ca_v\beta$ (24), are mediated by a ubiquitous, naturally abundant, and structurally different protein, CaM, but only on coexpression with α_{1C} and $\alpha_2\delta$. Recent image correlation spectroscopy measurements showed that *in vivo* CaM is sequestered in cells, and its availability for additional targeting is limited (25). This is consistent with our data showing that endogenous CaM is not sufficient for the $Ca_v\beta$-like modulation of the $Ca_v\beta$-free channel. An increase of local availability of CaM on overexpression (Fig. S1) may create conditions when CaM_{ex} targets specific $Ca_v\beta$-free conformations of the channel at different transient steps of assembly of the channel complex. Given that physiologically relevant variations of CaM expression do occur *in vivo* (26), a CaM_{ex}-like modulation of the channel may take place as a compensatory response. For example, this could explain a surprising observation (27) that knockout of the primary $Ca_v\beta_3$ gene in mouse ileum smooth muscle cells had little effect on I_{Ca} but did not change expression of $Ca_v1.2$ proteins.

The electrophysiological recordings indicated that, in the presence of $Ca_v\beta$, CaM_{ex} modulated $Ca_v1.2$ channels by increasing I_{Ca} amplitude, shifting maximum of the *I–V* curve to more negative voltages and facilitating (but not accelerating) inactivation (Fig. 1). In the absence of $Ca_v\beta$, $Ca_v1.2$ channels are silent, and the PM targeting by the $Ca_v\beta$-deficient complex is inhibited unless CaM_{ex} is coexpressed (Fig. 2*B*). The finding that β_{2d} and $CaM_{ex}/\alpha_2\delta$ are equipotent but not additive in the stimulation of the α_{1C} PM expression indicates that these different molecular entities may target the same mechanisms of the channel assembly and/or trafficking. However, amplitudes of the maximal I_{Ca} through $\alpha_{1C}/\alpha_2\delta/CaM_{ex/1234}$ channels (Figs. 2*D* and 4*B*) were ≈2 times smaller than that through $\alpha_{1C}/\alpha_2\delta/\beta_{2d}$ (Fig. 1*D*), suggesting that either electrophysiological properties or PM conformations of the channels (e.g., interaction with $\alpha_2\delta$) are different. Thus, unlike $Ca_v\beta$ or $\alpha_2\delta$, CaM_{ex} affects both the surface expression and gating of the channel. This bimodal regulation requires the presence of $\alpha_2\delta$ or $Ca_v\beta$, but is not associated with Ca^{2+}-binding activity of CaM_{ex} (Figs. 3 and 4). The latter suggests that Ca^{2+}/CaM-mediated signaling cascades and CDI are not involved, and that Ca^{2+}-dependent conformational changes of CaM_{ex} are not crucial for (but may affect) the gating of $Ca_v\beta$-free channels.

Experiments with expressed LA-IQ (2) have shown that folding and conformation of the LA-IQ region in the absence of $Ca_v\beta$ are strongly affected by CaM. It is also known that split LA and IQ motifs of the LA-IQ region bind CaM with different affinities. However, LA-IQ binds a single CaM when LA-IQ/CaM molar ratio is ≥1. This interaction, implicated for CDI, may be more complex in the native channel because of the binding of $Ca_v\beta$ to IQ (3) that may affect the CaM-dependent folding of LA-IQ and its affinity to CaM. We speculate that CaM_{ex} may exert its action on $Ca_v\beta$-free channels via interaction with $Ca_v\beta$-binding sites AID and/or LA/IQ in α_{1C}. Indeed, $Ca_v\beta$ inhibited binding of CaM_{ex} to $\alpha_{1C}/\alpha_2\delta$ (Fig. 5*A*). Mutation or deletion of known $Ca_v\beta$ sites in α_{1C} completely eliminated CaM_{ex}-dependent gating (Fig. 5 *B–E*), indicating that CaM_{ex} may target multiple interconnected determinants of α_{1C} associated with $Ca_v\beta$-subunit modulation of the channel. A mechanism consistent with our findings is that LA/IQ independently mediates both CDI and the effect of CaM_{ex} in the absence of $Ca_v\beta$, so that lack of the $Ca_v\beta$–IQ interaction in the $Ca_v\beta$-free channel may increase the probability of CDI-unrelated interaction(s) of CaM_{ex} with LA/IQ. Whether these interactions correspond to those observed in the laboratory of Hamilton and coworkers (28) remains to be seen. Finally, because $Ca_v\beta$, at least in part, inhibits these interactions (Fig. 5*A*), the augmentation of the current by CaM_{ex} (Fig. 1) may rely on a different set of interactions.

In conclusion, there is a functional matchup between CaM_{ex} and $Ca_v\beta$ that, in the absence of $Ca_v\beta$, renders PM targeting and gating of $Ca_v1.2$ channels via interaction with CaM molecule(s) other than the one tethered to LA/IQ to support CDI. Our results challenge the view that $Ca_v\beta$ subunits are indispensable for PM targeting and gating of $Ca_v1.2$ channels and raise the possibility that a similar $Ca_v\beta$-like modulation of PM targeting and gating by CaM may have place in other CaM-dependent Ca_v1 and Ca_v2 calcium channels (29, 30).

Materials and Methods

Expression in COS1 Cells. β_{2d} (31) was PCR-amplified from human cardiac polyA(+) mRNA and subcloned into a pcDNA3 vector. Because fusion with FLAG or ECFP/EYFP does not compromise functional properties of CaM (32) (see also Fig. S2) and $\alpha_{1C,77}$ (4), we used $ECFP_N$-CaM and the $FLAG_N$- or $EYFP_N$-tagged variants of human vascular α_{1C} ($\alpha_{1C,77}$) throughout experiments to ease detection and visualization of PM targeting by the channel. COS1 cells were grown on poly-D-lysine-coated coverslips 18 h before transfection with cDNAs coding for $\alpha_{1C,77}$, $\alpha_2\delta$, β_{2d}, and/or CaM (17) (1:1.2:1.4:5) using Effectene (Qiagen).

Electrophysiology. Whole-cell recordings were performed (20°C–22°C) 48–72 h after transfection as described in ref. 4 with an Axopatch200 B amplifier (Axon Instruments). The external solution was: 100 mM NaCl, 20 mM $CaCl_2$ (when recording I_{Ca}) or $BaCl_2$ (I_{Ba}), 1 mM $mMgCl_2$, 10 mM glucose, and 10 mM Hepes (pH 7.4), with NaOH. Patch pipettes had resistances of 2.5–4 MΩ when filled with an internal solution containing: 100 mM CsCl, 5 mM MgATP, 0.2 mM cAMP, 20 mM tetraethylammonium, 10 mM 1,2-bis(2-aminophenoxy)ethane-*N*,*N*,*N*′,*N*′-tetraacetate, and 20 mM Hepes (pH 7.4) with CsOH. Currents were filtered at 1 kHz, sampled at 2.5–5 kHz using pClamp 10 (Axon). Tail currents were filtered at 5 kHz and sampled at 13 kHz. Leak and capacitive transients were subtracted by using P/4 protocol. To achieve complete recovery from inactivation, test pulses were applied with 15-s intervals from $V_h = -90$ mV. Images were recorded with a Hamamatsu digital camera C4742–95 mounted on the Nikon epifluorescent microscope TE200 (60 × 1.2 N.A. objective) equipped with an excitation 75-W xenon lamp and multiple filter sets (Chroma Technology). Data were acquired and analyzed by using pClamp 10 (Axon) and Origin 7.5 (Microcal). Statistical analysis was performed with a unpaired

two-tailed Student's t test. All data are presented as mean ± SEM and considered significant if $P < 0.05$.

Protein Analyses. Assay of endogenous $Ca_v\beta$ subunits in COS1 cells was carried out as described in *SI Methods*. Monoclonal anti-β_1 (Neuromab) and polyclonal Ab to β_2, β_3, and β_4 (Millipore) were used for immunoblot analysis as described (7). Expressed proteins were solubilized, precleared with mouse IgG-agarose for 3 h, immunoprecipitated with anti-FLAG m_2 monoclonal affinity gel (Sigma), and resolved by SDS/PAGE. The specificity of our FLAG coIP system for $FLAG_N$-α_{1C} and $ECFP_N$-CaM is shown in Fig. S3.

ACKNOWLEDGMENTS. We thank Dr. J. M. Egan for critically reading the manuscript. This work was supported by the National Institute on Aging Intramural Research Program (Z01 AG000294-08, to N.M.S.).

1. Halling DB, Aracena-Parks P, Hamilton SL (2005) Regulation of voltage-gated Ca^{2+} channels by calmodulin. *Sci STKE* 2005:re15.
2. Xiong L, Kleerekoper QK, He R, Putkey JA, Hamilton SL (2005) Sites on calmodulin that interact with the C-terminal tail of $Ca_v1.2$ channel. *J Biol Chem* 280:7070–7079.
3. Zhang R, *et al.* (2005) A dynamic α-β intersubunit agonist signaling complex is a novel feedback mechanism for regulating L-type Ca^{2+} channel opening. *FASEB J* 19:1573–1575.
4. Kobrinsky E, *et al.* (2005) Differential role of the α_{1C} subunit tails in regulation of the $Ca_v1.2$ channel by membrane potential, β subunits, and Ca^{2+} ions. *J Biol Chem* 280:12474–12485.
5. Shi C, Soldatov NM (2002) Molecular determinants of voltage-dependent slow inactivation of the Ca^{2+} channel. *J Biol Chem* 277:6813–6821.
6. Peterson B, *et al.* (2000) Critical determinants of Ca^{2+}-dependent inactivation within an EF-hand motif of L-type Ca^{2+} channels. *Biophys J* 78:1906–1920.
7. Kobrinsky E, *et al.* (2004) Voltage-gated rearrangements associated with differential β-subunit modulation of the L-type Ca^{2+} channel inactivation. *Biophys J* 87:844–857.
8. Kobrinsky E, Schwartz E, Abernethy DR, Soldatov NM (2003) Voltage-gated mobility of the Ca^{2+} channel cytoplasmic tails and its regulatory role. *J Biol Chem* 278:5021–5028.
9. Pragnell M, *et al.* (1994) Calcium channel β-subunit binds to a conserved motif in the I-II cytoplasmic linker of the α_1-subunit. *Nature* 368:67–70.
10. Peterson BZ, DeMaria CD, Adelman JP, Yue DT (1999) Calmodulin is the Ca^{2+} sensor for Ca^{2+}-dependent inactivation of L-type calcium channels. *Neuron* 22:549–558.
11. Pitt GS, *et al.* (2001) Molecular basis of calmodulin tethering and Ca^{2+}-dependent inactivation of L-type Ca^{2+} channels. *J Biol Chem* 276:30794–30802.
12. Zühlke RD, Pitt GS, Deisseroth K, Tsien RW, Reuter H (1999) Calmodulin supports both inactivation and facilitation of L-type calcium channels. *Nature* 399:159–162.
13. Saimi Y, Kung C (2002) Calmodulin as an ion channel subunit. *Annu Rev Physiol* 64:289–311.
14. Meir A, Bell DC, Stephens GJ, Page KM, Dolphin AC (2000) Calcium channel β subunit promotes voltage-dependent modulation of α1B by G$\beta\gamma$. *Biophys J* 79:731–746.
15. Neely A, Olcese R, Wei XY, Birnbaumer L, Stefani E (1994) Ca^{2+}-dependent inactivation of a cloned cardiac Ca^{2+} channel α_1 subunit (α_{1C}) expressed in *Xenopus* oocytes. *Biophys J* 66:1895–1903.
16. Leroy J, *et al.* (2005) Interaction via a key tryptophan in the I-II linker of N-type calcium channels is required for β1 but not for palmitoylated β2, implicating an additional binding site in the regulation of channel voltage-dependent properties. *J Neurosci* 25:6984–6996.
17. Romanin C, *et al.* (2000) Ca^{2+} sensors of L-type Ca^{2+} channel. *FEBS Lett* 487:301–306.
18. Soldatov NM, Oz M, O'Brien KA, Abernethy DR, Morad M (1998) Molecular determinants of L-type Ca^{2+} channel inactivation. Segment exchange analysis of the carboxyl-terminal cytoplasmic motif encoded by exons 40–42 of the human α_{1C} subunit gene. *J Biol Chem* 273:957–963.
19. Soldatov NM, Zühlke RD, Bouron A, Reuter H (1997) Molecular structures involved in L-type calcium channel inactivation. Role of the carboxyl-terminal region encoded by exons 40–42 in α_{1C} subunit in the kinetics and Ca^{2+} dependence of inactivation. *J Biol Chem* 272:3560–3566.
20. Zühlke RD, Reuter H (1998) Ca^{2+} sensitive inactivation of L-type Ca^{2+} channels depends on multiple cytoplasmic amino acid sequences of the α_{1C} subunit. *Proc Natl Acad Sci USA* 95:3287–3294.
21. Chen Y-h, *et al.* (2004) Structural basis of the α_1-β subunit interaction of voltage-gated Ca^{2+} channels. *Nature* 429:675–680.
22. Opatowsky Y, Chen C-C, Campbell KP, Hirsch JA (2004) Structural analysis of the voltage-dependent calcium channel β subunit functional core and its complex with the α1 interaction domain. *Neuron* 42:387–399.
23. Van Petegem F, Clark KA, Chatelain FC, Minor DL, Jr (2004) Structure of a complex between a voltage-gated calcium channel β-subunit and an α-subunit domain. *Nature* 429:671–675.
24. Dolphin AC (2003) β Subunits of voltage-gated calcium channels. *J Bionenerg Biomembr* 35:599–620.
25. Sanabria H, Digman MA, Gratton E, Waxham MN (2008) Limiting calmodulin revealed by image correlation spectroscopy. *Biophys J* 94:92.
26. Abzhanov A, *et al.* (2006) The calmodulin pathway and evolution of elongated beak morphology in Darwin's finches. *Nature* 442:563–567.
27. Held B, *et al.* (2007) Ca^{2+} channel currents and contraction in $Ca_v\beta_3$-deficient ileum smooth muscle from mouse. *Cell Calcium* 42:477–487.
28. Tang W, *et al.* (2003) Apocalmodulin and Ca^{2+} calmodulin-binding sites on the $Ca_v1.2$ channel. *Biophys J* 85:1538–1547.
29. Lee A, *et al.* (1999) Ca^{2+}/calmodulin binds to and modulates P/Q-type calcium channels. *Nature* 399:155–159.
30. Liang H, *et al.* (2003) Unified mechanisms of Ca^{2+} regulation across the Ca^{2+} channel family. *Neuron* 39:951–960.
31. Colecraft HM, *et al.* (2002) Novel functional properties of Ca^{2+} channel β subunits revealed by their expression in adult rat heart cells. *J Physiol* 541:435–452.
32. Miyawaki A, *et al.* (1997) Fluorescent indicators for Ca^{2+} based on green fluorescent proteins and calmodulin. *Nature* 388:882–887.
33. Lao QZ, Kobrinsky E, Harry JB, Ravindran A, Soldatov NM (2008) New determinant for the Cavβ2-subunit modulation of the Cav1.2 calcium channel. *J Biol Chem*, in press.